This is the Pre-Published Version.
F. Richter, F.X. Jervis, X. Huang, G. Rein (2021) *Effect of Oxygen on the Charring Rate of wood*, **Combustion and Flame**, 234, 111591. doi: 10.1016/j.combustflame.2021.111591

Effect of Oxygen on the Burning Rate of wood

Franz Richter[1,2], Freddy X. Jervis[3], Xinyan Huang[4], and Guillermo Rein[1]*

[1]Department of Mechanical Engineering, Imperial College London, UK.

[2]Department of Mechanical Engineering, University of California at Berkeley, USA.

[3]Faculty of Mechanical Engineering and Production Sciences, Escuela Superior Politecnica del Litoral (ESPOL), Guayaquil, Ecuador.

[4]Department of Building Services Engineering, Hong Kong Polytechnic University, HK.

Abstract

The large-scale adoption of wood as a construction material for commercial buildings could pave the way for a sustainable construction industry. Its adoption, however, is hindered by a limited understanding of wood's burning behaviour. The roles of oxygen and smouldering combustion are deemed significant but have not been quantified. We address this shortcoming by studying the effect of oxygen concentration and other variables on the burning behaviour of particleboard experimentally and computationally. We conducted over 60 experiments on cm-scale samples of particleboard spanning different oxygen concentrations (0-21 %), heat fluxes (10-70 kW/m^2), densities (600 – 800 kg/m^2), and sample thicknesses (6 -25 mm). Only the heat flux and oxygen concentration significantly affect the burning rate (mass flux in pyrolysis), time-to-flaming ignition, and burning mode. To explore this effect further, we developed a computational model of particleboard burning in Gpyro. Combing the computational and experimental results, we show that particleboard undergoes only pyrolysis below 4 % oxygen, smouldering between 4 and 15 %, and flaming above 15 %. These oxygen thresholds were found to decrease as the heat flux increases and vice versa. Both flaming and smouldering increase the burning rate to a similar degree (37 and 25 %) compared to pyrolysis in an inert atmosphere. This means that the rate of loss of section of structural wood in fire due to smouldering could be similar to that by flaming combustion. In addition, we observed, for the first time, a triple point for the ignition of wood at which a small change in environmental conditions can lead to either smouldering, flaming, or pyrolysis. Near this triple point, smouldering is likely to be a hidden catalyst for flaming. Current design methodologies ignore smouldering and this inaccuracy could potentially be unsafe. In summary, this paper quantifies for the first time the contributions of the three combustion regimes of wood, highlights the importance of smouldering, and provides a novel dataset for future studies.

Keywords: Timber; Biomass; Fire; Smouldering; Charring

Nomenclature

A	pre-exponential factor (1/s)	z	distance (mm)
c	heat capacity (J/kg-K)	n_{O_2}	Oxygen reaction order (-)
E	activation energy (J/mol)	$[O_2]_a$	ambient oxygen concentration (%)
h	Enthalpy (J)	$[O_2]_s$	surface oxygen concentration (%)
h_c	convective coefficient (W/m^{2}s)	***Greeks***	
h_m	Mass transfer coefficient (kg/m^2-s)	ε	emissivity (-)
ΔH	heat of reaction (kJ/mol)	ρ	bulk density (kg/m^3)
k	thermal conductivity (kg/m^3)	v	Viscosity (m^2/s)/stoichiometry or solid
K	Permeability (m^2)	ρ_{so}	solid density, $\rho/\rho_s=1-\Phi$
$\dot{m}''$	mass flux (g/m^2-s)	Φ	porosity (-)
n	heterogeneous reaction order (-)	$\dot{\omega}'''$	volumetric reaction rate (kg/m^3-s)
P	Pressure (Pa)	***Subscripts***	
$\dot{q}''$	heat flux (kW/m^2)	0	Initial
R	universal gas constant (J/mol-k)	g	gas
t	Time (s)	i	condensed species number
T	Temperature (°C)	j	gaseous species number
Y	mass fraction (g/g)	k	reaction number
		O_2	local oxygen
		aO_2	ambient oxygen

1 Introduction

Engineered wood is becoming a popular construction material due to its beauty, cost-efficiency, and sustainability [1]. It is made through gluing wood fibres (Medium Density Particleboard), chips (Low Density Particleboard), or planks (Cross Laminated Timber) together in various ways depending on the desired properties. A limited understanding of the burning behaviour of engineered wood, however, hinders its uptake [1]. We explore the burning behaviour of particleboard as a surrogate for engineered woods.

Previous studies have investigated engineered and raw wood at the micro- (≤mg-samples) and mesoscale (≤g-samples) [2–5]. They explored the pyrolysis [3,6], the cracking behaviour [7], the flaming ignition [8], and flame spread [4]. These studies, however, have not characterised the burning behaviours of particleboard at a fundamental level as only a single oxygen concentration was studied. The burning behaviour of a polymer (particleboard is to 90 % a natural polymer) depends on the oxygen concentration in the surrounding atmosphere [8]. Current studies on flame spread and ignition of fibreboard [4,9]—the closest studied material in the literature to particleboard—have focused on the burning behaviour in air, where flaming ignition (of wood) occurs within minutes at heat fluxes beyond 12 kW/m^2 [8]. Some studies on the fire resistance of structural wood (timber) are conducted in furnaces where the oxygen concentration near the sample surface are below 8 % [10]. At such low oxygen concentration, flaming would not be expected to take place, and instead, a polymer is only expected to extinguish or only smoulder [11–13].

Smouldering is the low temperature and flameless heterogeneous combustion of solid [12]. In the complete absence of oxygen, a polymer will only undergo pyrolysis without any oxidation. In other words, different oxygen concentrations are expected to give rise to different modes of combustion (Fig. 1). Each of these presents its own unique hazard. For example, a flaming fire propagates faster through a room but is easier to extinguish than a smouldering fire. Under the right conditions, any of these fire modes (pyrolysis, smouldering, flaming) can transition to another in an unpredictable manner [12]. In building fires, the oxygen concentration varies across the building, and all modes are expected to take place, so that it is important to understand them and their transition. Although several work studied the critical external radiation for wood flaming extinction [14,15], to date few studies have yet investigated the critical conditions (especially oxygen concentration) for wood for these fire modes to take place [11,16–19]. Moreover, even fewer studies have quantified the relative contribution of each fire mode under different conditions, which is the first step to unravel the dangerous transition between different fires.

In this study, we aim to characterize the effect of oxygen concentration and other variables on the burning behaviour of particleboard. The other variables are heat flux, sample thickness, and density, which have been speculated or shown to affect the burning behaviour of wood [8,20].

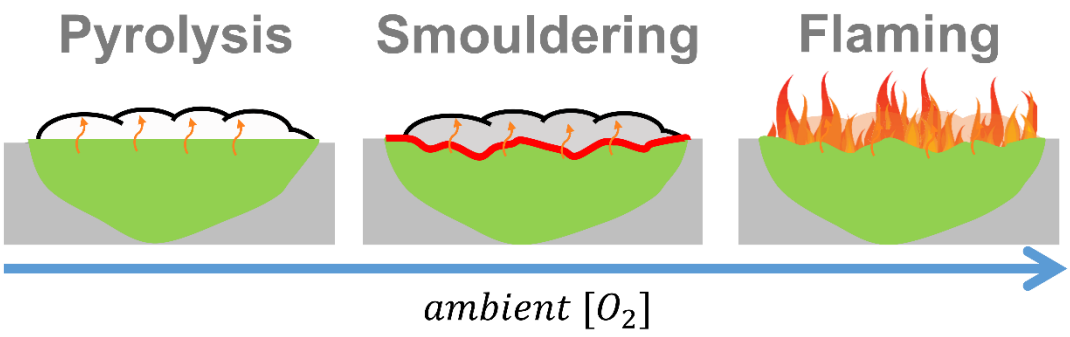

Fig. 1 Three modes of burning (pyrolysis, smouldering, flaming) as a function of ambient oxygen concentration. Pyrolysis supplies the fuel for smouldering and flaming and is the first step in the burning of wood. Flaming and smouldering both have the potentially to unexpectedly transition between each other.

2 Experimental and Computational Method

2.1 Experimental Methods

The experiments were conducted using the FM-Global Fire Propagation Apparatus (FPA) following ASTM E 2058 combustion test. In an FPA, the fuel sample is exposed to a radiative heat flux, and a pilot ignition source is placed above its free surface. In this study, the range of radiative heat imposed was varied from 10 to 70 kW/m^2 and maintained constant for the whole duration of the experiment. The sample mass was measured, and the exhaust gases were analysed for composition, temperature, and flow rate. The ambient conditions were controlled through an imposed flow of oxygen concentrations ranging from 0 to 21 %. The flow speed was set to 200 L/min based on the standard.

The sample size studied was 8 by 8 cm with different thicknesses with its unexposed sides surrounded by 3 layers of thick cotronics ceramic paper (3mm each) to minimise heat losses to the sides and back of the sample. The sample was then pushed into a metallic holder and placed on the stand of the mass balance. Measurements were obtained following ASTM E 2058, the standard practice for using the FPA, combustion test. The Heat Release Rate was obtained through the carbon dioxide and carbon monoxide generation method as discussed in detail in [21]. The mass flux was obtained through differentiating and smoothing the measured mass over time. The burning rate was then assumed equal to the mass loss rate in the combustible atmosphere. Table S1 lists all experiments of particleboard of different densities and different thicknesses at different heat fluxes and oxygen concentrations conducted.

2.2 Computational model formulation, mesh, and input parameters

We developed a generalised pyrolysis model of particleboard in Gpyro [22] consisting of a chemical kinetics and transport model as these are some of the processes that affect the burning of timber as shown in Fig. 3. The process of cracking and delamination are not considered here, as we particleboards are non-laminated (does not delaminate) and cracking was not found significant in our experiments.

The chemical kinetics, both reaction scheme and kinetic parameters, of wood were taken from [23], with the reaction scheme shown in Fig. 2.

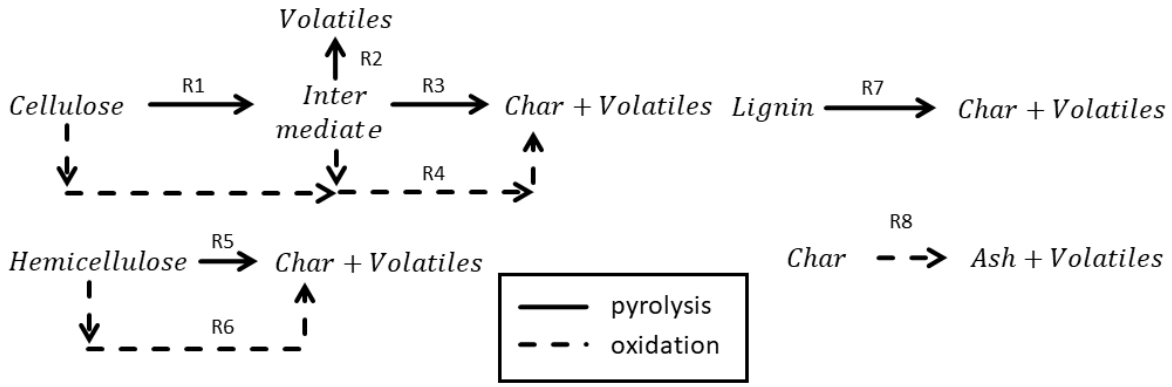

Fig. 2 Sketch of Reaction scheme from [24]

The consumed oxygen for pyrolysis reactions (R1-R3,R5,R7) is 0, for fuel oxidation (R4 & R6) reactions 0.41 g/g-fuel [25], and for char oxidation (R8) reactions six times the amount of fuel oxidation (2.46) [26]. The heat of reactions are taken from [23,25,27] as discussed later. The reaction scheme is the linear superposition of wood's three main components: cellulose, hemicellulose, and lignin. It consists of 5 pyrolysis reactions, 2 fuel oxidation reactions, 1 char oxidation reaction, and 6 solid species (cellulose, hemicellulose, lignin, intermediate, char, and ash). The respective ratio of cellulose, hemicellulose, and lignin is assumed fixed as 0.459,0.251, and 0.29, respectively [28]. The measured moisture sample was around 5 %, which was deemed insufficient to include a drying model.

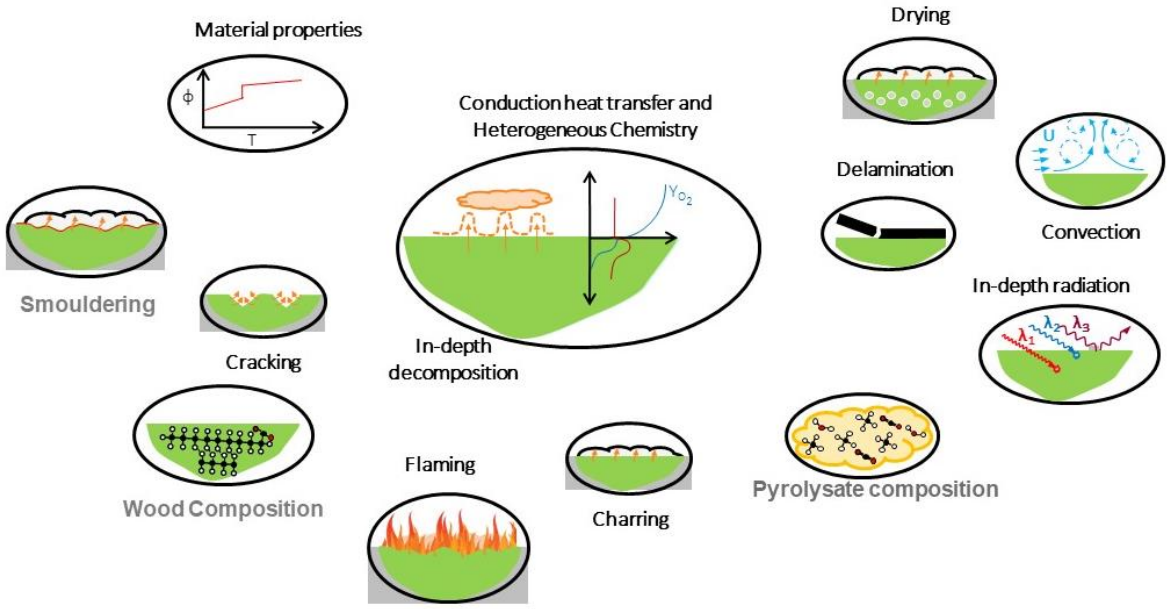

Fig. 3 Sketch of the different chemical, physical, and mechanical processes that affect the burning rate of timber. The process of cracking and delamination are not considered here, as we particleboards are non-laminated (does not delaminate) and cracking was not found significant in our experiments.

The rate of pyrolysis and oxidation reactions can be described by Eq. (1)

$$\dot{\omega}_i''' = \bar{\rho} Y_{A,k} Y_{O_2}^{n_{O_2 k}} A_k \exp(-E_k/RT) \quad (1)$$

This kinetic model is incorporated into Gpyro, which solves the main five one-dimensional conservation equations for condensed-phase mass (2), species (3), and energy (4), and those for the gas-phase mass (5), species (6), and momentum (7):

$$\frac{\partial \bar{\rho}}{\partial t} = -\dot{\omega}_{fg}''' \quad (2)$$

$$\frac{\partial (\bar{\rho}\, Y_i)}{\partial t} = \dot{\omega}_{fi}''' - \dot{\omega}_{di}''' \quad (3)$$

$$\frac{\partial (\bar{\rho}\bar{h})}{\partial t} = k \frac{\partial}{\partial z}\left(\frac{\partial T}{\partial z}\right) + \dot{\omega}_{fi}'''(-\Delta H_i) \quad (4)$$

$$\frac{\partial}{\partial t}(\rho_g \bar{\phi}) + \frac{\partial \dot{m}''}{\partial z} = \dot{\omega}_{fg}''' \quad (5)$$

$$\frac{\partial}{\partial t}(\rho_g \bar{\phi} Y_j) + \frac{\partial}{\partial z}(\dot{m}'' Y_j) = -\frac{\partial}{\partial z}\left(\bar{\phi}\rho_g D \frac{\partial Y_j}{\partial z}\right) + \\ + \dot{\omega}_{fj}''' - \dot{\omega}_{dj}''' \quad (6)$$

$$\dot{m}'' = -\frac{\kappa}{\nu}\frac{\partial p}{\partial z} \quad (7)$$

The overbar represents the respective mass or volume average. The mesh size was 0.1 mm, and the time step was 0.1 s. All material properties were taken from the literature and given in Table 1. The pore diameter d_p was calculated from the density [29], the permeability was found from the pore diameter [29], and the radiative conductivity component from the emissivity and pore diameter [2].

*Table 1 Material properties used in this study. Quantities denoted with the sign # indicate calculations and * indicated measurements*

Species (i)	ρ_i (kg/m^3)	k_i (kg/m^3)	c_i (J/kg-K)	ε (-)	γ (mm)	ρ_{soi} (kg/m^3)	K x 10^{10} (m^2)	d_p (mm)
Timber	630*	0.189 [2]	2300 [5]	0.7[30]	0.612#	1513[31]	0.01#	0.03#
Char	220#	0.117 [2]	1100 [5]	0.95[5]	1.29#	1467[5]	0.083#	0.09#
Ash	18.9#	0.8 [32]	880 [32]	0.95[32]	3.76#	2500[32]	0.7#	2.65#

2.3 Boundary condition

The boundaries of the sample consist of a free surface at z=0 and an insulated surface z=δ, as shown in Fig. 4 a. At the back surface ($z = \delta$), we assume that the surface is adiabatic (h=0) and impermeable ($\frac{dP}{dt} = 0$). At the front surface (z=0) we assume $h = 10$ W/m^2-s [9] and a mass transfer coefficient of $h_m = 0.01$ kg/m^2-s, the heat flux as defined in Eq. (8):

$$\dot{q}_{inc}'' = \begin{cases} \dot{q}_{ir} & [O_2]_a < 15\ \% \\ \dot{q}_{ir} + \dot{q}_f & [O_2]_a > 15\ \%\ \ t_{ig} < t < t_{fl} \end{cases} \quad (8)$$

where $\dot{q}_{ir}$ is the irradiation from the heater, $\dot{q}_f$ the flaming heat flux, and $\dot{q}_{inc}$ the incident heat flux on the sample surface. The flaming heat flux is fitted based on experimental measurement, as $\dot{q}_f = 137 Y_{aO_2}^{1.3}$, where Y_{aO_2} is the ambient oxygen mass fraction. Y_{aO_2} is calculated from $[O_2]_a$ assuming the split of oxygen and nitrogen at standard conditions in air. This correlation is based on [33] and a heat flux of 20 kW/m^2 in air [9]. Note that the flaming heat flux has a growth period of 70 s and a decay period in the last 170 s before extinction (Fig. 5), according to the experiment in [9]. Notably, particleboard shows a parabolic non-uniform density profile, which is defined based on the medium density and ratio of minimum to maximum density (ρ_{max}/ρ_{min}) in the sample [6]. For particleboard, we measured that density ratio to be 2 by measuring the density of individual slices of different depths (Fig. 4 b). Such a parabolic shape was modelled in Gpyro by 18 discrete density layers [9].

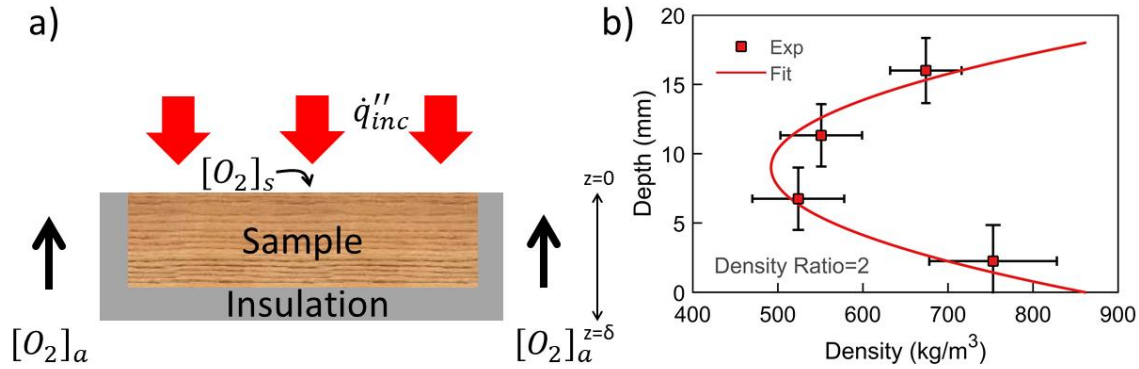

Fig. 4 a) Sketch of oxygen flow and irradiation to the sample. b) Comparison between measured and fitted density profile of the particleboard

In Eq. (1) the local oxygen concentration Y_{O_2} is used to calculate the the reaction rate. Y_{O_2} in turn is determined via Eq. (6) using as a boundary conditions the oxygen concentration of the sample surface and heat transfer coefficient. Due to the presence of a flame the oxygen concentration at the surface differs from the ambient oxygen concentration and is calculated in Eq. (9).

$$[O_2]_s = \begin{cases} [O_2]_a & [O_2]_a < 15\ \% \\ f(\mathrm{CR}) & [O_2]_a > 15\ \% \end{cases} \quad (9)$$

The function $f(CR)$ is calculated in Eq (10).

$$[O_2]_s = f(\mathrm{CR}) = \frac{\mathrm{CR}([O_2]_a) - \mathrm{CR}_{\min}}{\mathrm{CR}_{max} - \mathrm{CR}_{min}} [O_2]_a \quad (10)$$

where CR is the measured CO/CO$_2$ ratio and stands for carbon ratio, CR_{min} is the minimum measured CO/CO$_2$ ratio for smouldering without flame, and CR_{max} is the maximum measured CO/CO$_2$ ratio for a strong flame. A comparison between the predictions of $[O_2]_s$ with Eq. (10) and experimental data is illustrated in Fig. 6. Good agreement was observed across all oxygen concentrations.

In other words, we know for certain that below 15 % $[O_2]_a$ we have no flame and only smouldering present, and that at 21 % $[O_2]_a$ we only have flaming present. At 15<$[O_2]_a$< 21 %, there is either some

smouldering, some flaming, or mix present. This mixture is calculated by interpolation, which is analogous to the concepts of the modified combustion efficiency (MCE) that has been previously used to assess the relative contribution of flaming and smouldering during burning of solids [34]. The idea of the MCE is that the lower the value, the larger the amount of CO released, the more incomplete the combustion, and hence, the weaker the flame. This idea was used in Eqn (10) to estimate the amount of oxygen arriving at the solids surface in the presence of a flame, as a stronger flame is expected to consume more oxygen and release less CO than a weaker flame. Notably, we took CR_{min} at 12 % $[O_2]_a$, as some studies report flaming at around 15 % [16,17] and we wanted to ensure to choose a value of CR_{min} away from the transition point between flaming and smouldering. Choose the CR_{min} at 15 % would result in an 8 % change in CR_{min} value. Furthermore, the above was expressed in CR instead of MCE (=1/(1+CR)) as we found better agreement using CR than MCE with the experimental data. MCE predicts a higher $[O_2]_a$ than CR. Fig. 6 compares the experimentally measured values of the surface oxygen concentrations with those calculated by Eq. (10). In addition, the rate of supply of oxygen from the ambient to the surface exceeds the rate of consumption of oxygen by smouldering, so that the concentration of oxygen at the surface is constantly around the ambient value in the absence of a flame.

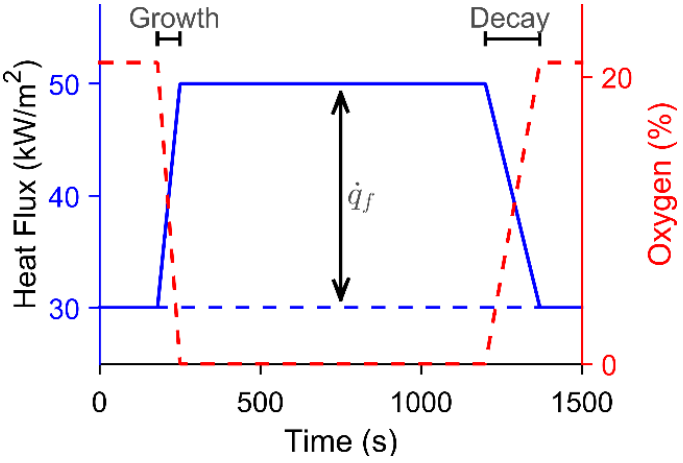

Fig. 5 Sketch of the time evolution of the applied heat flux and oxygen concentration at the surface of a sample under a constant irradiation of 30 kW/m² and 21 % ambient oxygen.

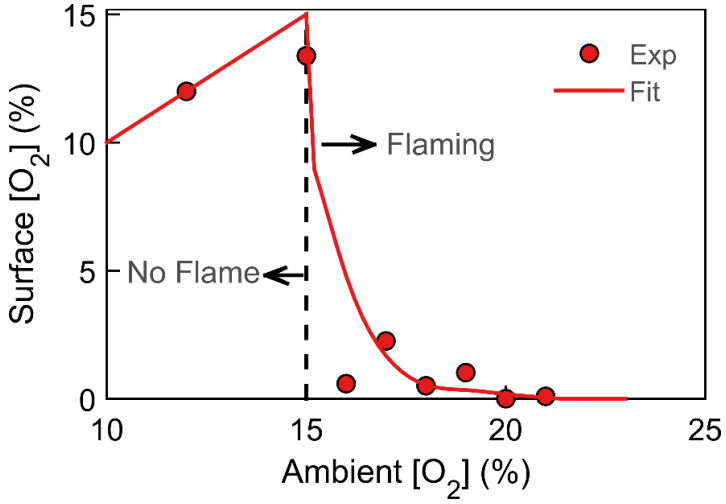

Fig. 6 Dependence of surface oxygen concentration on ambient oxygen concentration with a criticality at 15 % for flaming.

3 Results and Discussion

3.1 Model validation and analysis

The model was developed at the microscale and mesoscale against several experiments based on our previous work on natural wood [23,28]. Engineered wood differs from natural wood due to the presence of resin (affects kinetic model and heat of reactions), absence of grain direction (thermal conductivity), density gradient (density), and porosity gradient (porosity, pore diameter). We found the resin to have an insignificant influence on the chemical kinetics as our chosen kinetic model performs well against the experiments of MDF [9]—closest related material studied in the literature—at the microscale (error=1.1σ_e in mass loss history). At the mesoscale, we further found that the heat of reactions and coefficient of oxygen consumption of natural wood perform well for particleboard as well. This conclusion was drawn from a sensitivity study and comparison to the experiments of 18 mm particleboard at 0 and 12 % (Fig. 7 a & b, error=1.05 σ_e). Following the sensitivity analysis, the heat of reaction of the fuel oxidation of hemicellulose (R6) was set to zero due to its insignificant influence across the whole literature range. We accounted for the absence of grain direction in particleboard by using a thermal conductivity of wood and char that resembles closely the average thermal conductivity ($k = 0.189$ W/m-K) [35] of wood across all three grain directions ($k \approx 0.2$ W/m-K) [2].

Particleboard is known to have a density gradient, which was measured in Section 2.3. A density gradient implies a porosity and permeability gradient. We accounted for this effect by making the porosity ($\phi = 1 - \rho/\rho_{s0}$) of particleboard dependent on the bulk density (ρ) through a constant solid density (ρ_s). That is, the pore diameter is a function of bulk density, and the permeability is a function of the pore diameter. A sensitivity study reveals that the model is insensitive to the exact value of these parameters, while a comparison with experiments (Fig. 8, Fig S1 for rotated form) showed good agreement (error=1.16σ_e).The largest errors, up to 6.3σ_e, are observed at low heat fluxes (below 20 kW/m^2). Thus, the model is suitable to investigate the fundamental processes of burning particleboard.

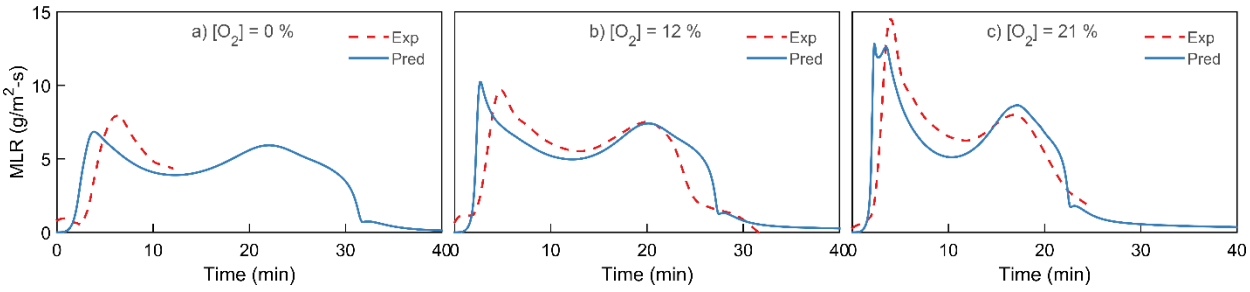

Fig. 7 Comparison between experiments and predictions at three oxygen concentrations at 30 kW/m^2 of an 18 mm thick sample.

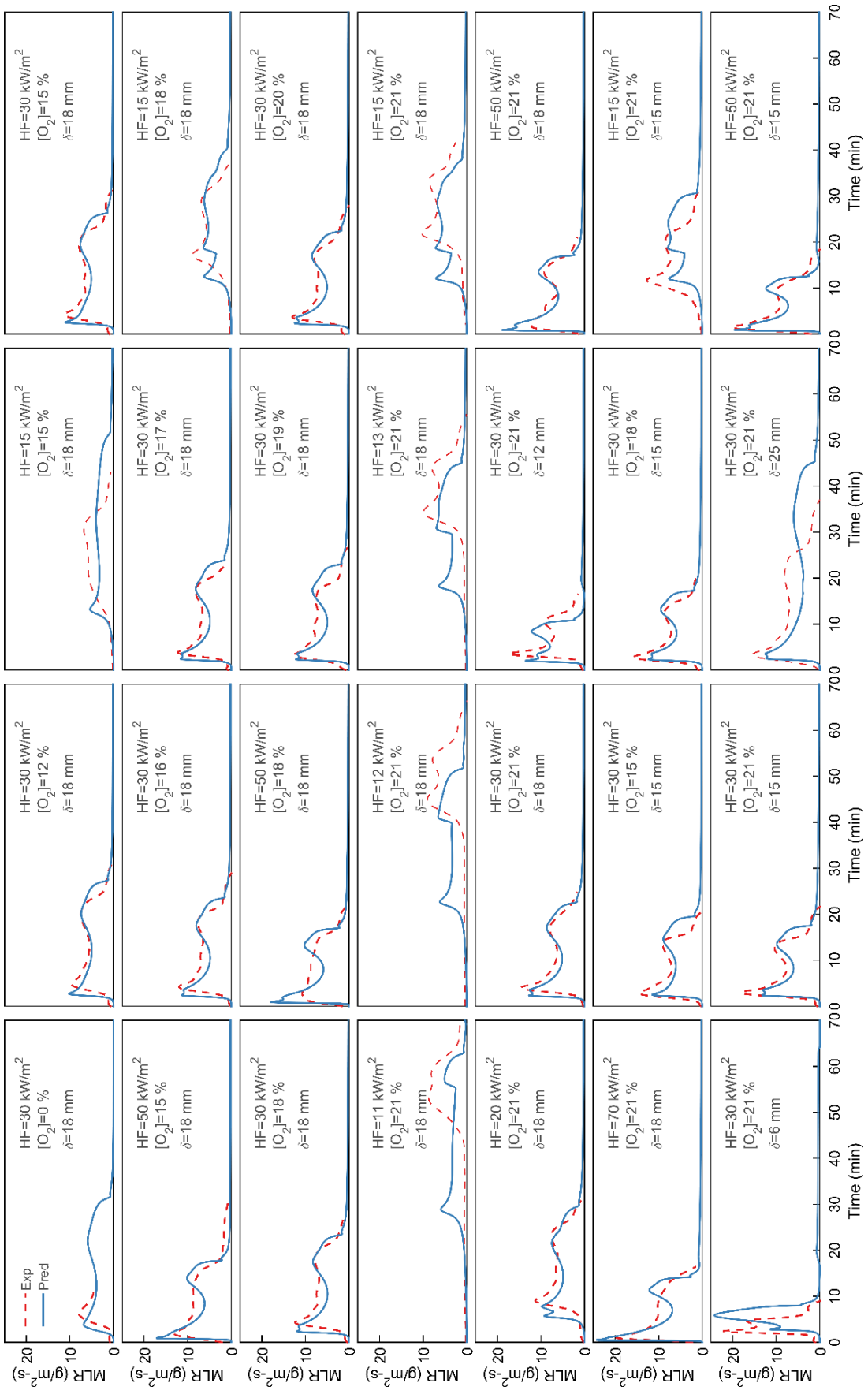

Fig. 8 Comparison between all unique experiments, in terms of conditions, and the prediction

3.2 Mass loss rate and limiting oxygen concentration

Modelling results reveal that the oxygen concentration controls the mode of burning for particleboard. Specifically, under the heat flux of 30 kW/m^2, pyrolysis dominates below 4% $[O_2]_a$, while smouldering between 4% and 15% $[O_2]_a$, and flaming above 15% $[O_2]_a$. Fig. 9 compares the predicted average mass loss rate with the measured average mass loss rate, where predictions are within the experimental uncertainty, showing an excellent agreement. It is well established in the literature that there are three modes of burning (pyrolysis, smouldering, and flaming) for any charring material, which are significantly influenced by the oxygen concentration [11]. Pyrolysis is the thermal degradation of biomass that does not require oxygen. Smouldering is the low temperature heterogeneous combustion of biomass [36]. Within this study, we defined the boundary of smouldering by the threshold of a propagating char oxidation reaction. Flaming is the homogeneous combustion of volatiles.

Based on our model predictions, we found that below 4 % $[O_2]_a$, only pyrolysis and fuel oxidation reactions take place. The oxidation of char is restricted to the surface and cannot form a propagation, so that we concluded that under these conditions, the burning is controlled by pyrolysis. Only above 4 % $[O_2]_a$, the oxidation of char becomes significant and starts to travel into the solid. Note that this limiting oxygen concentration will increase as the external radiation decreases. This fact manifests itself in the model through a large uncertainty (red cloud, Fig. 9) in the model that is driven by the uncertainty in the heat of char oxidation. Around 15 %, we experimentally observed the appearance of a flame or flashes (Fig. 9) from which we conclude that this is the point of the criticality of flaming under given external radiation (30 kW/m^2). The appearance of a flame coincidence with the ceasing of smouldering during the period of flaming (lasting 850 s). Smouldering ceases due to the consumption of oxygen by the flame above the solid, which we also confirmed computationally by seeing no smouldering reaction during the flaming period (Fig S2).

The discovered limiting oxygen concentration of flaming under the external radiation (14 – 15 % for wood) agrees well with the literature where the PU Foam was found to transition from smouldering to flaming above 17 % $[O_2]_a$ [37]. Plastics were found to support sustained flaming above 14 – 16 % $[O_2]_a$ depending on the pressure [33] and external radiation [13], and moss was found to ignite by flaming above 15 % $[O_2]_a$ [17]. Similarly, our criticality of smouldering agrees well with the literature where self-sustained smouldering was found to require 10 % O_2 [38], but aided smouldering only 5 % $[O_2]_a$ [19] which is close to our threshold of 4 %.

The average mass loss rate in all three modes of burning is of the same magnitude, which means that each mode poses a hazard. For example, the burning rate of particleboard at 20 % $[O_2]_a$ is only double that at 10 % $[O_2]_a$. For wood structural component (timber), its fire performance is evaluated by the charring rate (speed of pyrolysis front) [20] which is proportional to the burning rate/mass loss rate. A smouldering timber member would also experience a significant charring rate, comparable to a flaming timber member. This finding could explain the significant strength-loss [20] after flaming has ceased, as observed in fire tests of timber (referred to as the cooling phase) [39]. Wiesner et al. [39]

showed that this strength loss during the ''cooling'' phase of a fire is not incorporate in current fire safety designs and highlighted the subsequent increased risk. Our findings here support the hypothesis that strength loss of timber can be significant in the absence of flaming due to smouldering driven combustion. In fact, the visuals of Kinjo et al. [40] showed a glowing timber beam after a fire test, which indicated a robust smouldering. This evidence provides a case for an increasing need to examine smouldering in more detail for timber structures, as originally proposed elsewhere [41].

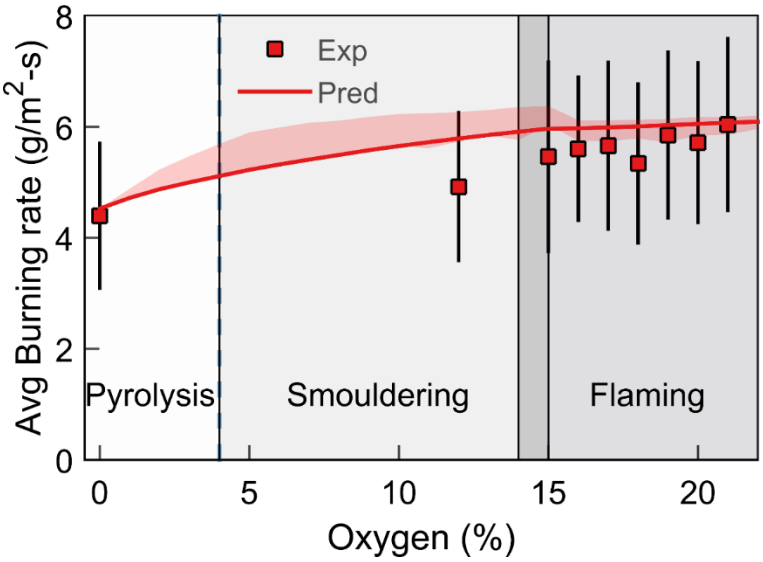

Fig. 9 Average burning against oxygen for a low density fibre board sample of 18 mm at a constant heat flux of 30 kW/m^2 for a time of 1500 s (average running time of the experiments). The red cloud represents the model uncertainty.

3.3 Ignition thresholds for wood

The burning behaviour of wood is influenced by both oxygen concentration and heat flux. Figure 10 shows the Ignition Diagram for wood that describes the effect of oxygen and heat flux on the burning mode of wood. As described in Section 3.2, there are two ignition thresholds for wood: one for smouldering combustion and one for flaming combustion. The limiting oxygen concentration decreases for both them as the heat flux increases. A similar phenomena has previously been observed for flame spread over plastics [42] and for the extinction of wood [18]. Comparing our experimental measurements for the flaming ignition of wood with those for flaming extinction of wood by Cuevas et al. [18] suggests that the threshold for ignition and extinction of wood differ. From this comparison, we conclude that our data should only be treated as ignition thresholds for flaming and smouldering. They may not hold for extinction.

Our ignition diagram reveals for the first point a triple point for the ignition of wood at a heat flux of 22.22 kW/m^2 and an oxygen concentration of 17.15 %. Near this triple point a small change in the condition can result in either pyrolysis, flaming, or smouldering. We can further conclude that the fire risk near this triple point is disproportionately large to the expected risk. Crossing the smouldering ignition threshold near this triple point is likely to lead to an increase in heat flux from the additional

heat from smouldering, which would then cause the crossing of the flaming threshold. Meaning that near the triple point the flaming threshold is effectively lower than anticipate when smouldering is neglected. This point highlights the importance of considering smouldering combustion as a fire safety hazard when dealing with wood e.g. in timber construction, wood storage, or wildfires. Smouldering combustion presents a danger in itself (Section 3.3) and as a catalyst for flaming combustion.

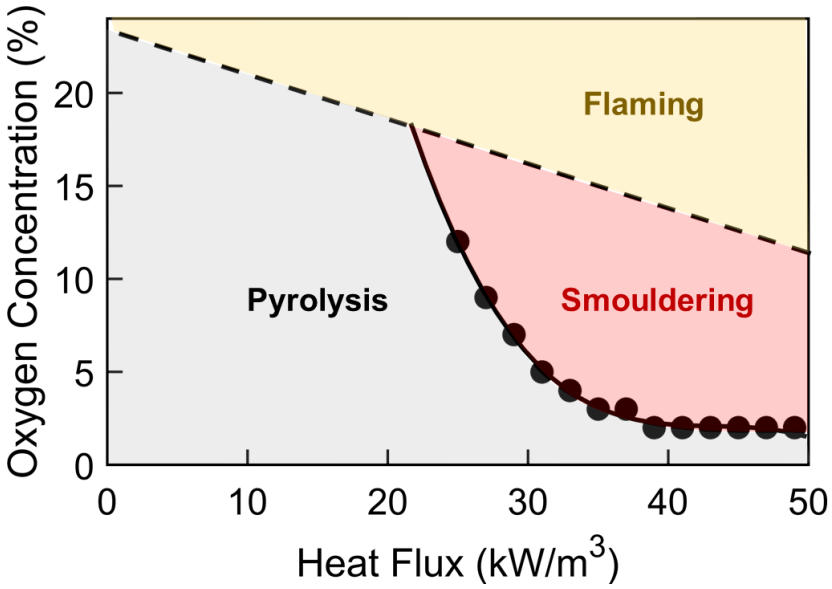

Figure 10 Influence of oxygen and heat flux on the ignition thresholds for timber. The flaming threshold is based on experimental measurements at 13, 15, and 30 kW/m^2. The smouldering threshold is based on simulations. Notably the threshold only holds for ignition, which means going either right on the graph or upwards.

3.4 Other influence parameters

Fig. 11 a & d show that the burning rate increases and time-to-flaming ignition decrease with heat flux as was expected [43]. The critical heat flux for flaming ignition was found to be 10 kW/m^2 (Fig. 11 a), and the critical mass loss rate was around 10 g/m^2-s (Fig. 11 g), which is in line with the literature [9,43]. The latter was found to be constant across different densities and thicknesses. Surprisingly, we found experimentally that density and sample thickness (Fig. 11 b&c) did not affect the burning rate at 30 kW/m^2 in air. The model does predict a slight increase in burning rate with density (Fig. 11 b), as would be expected, but such trend is within the experimental errors. Thus, the density influence (1.6 g/m^2-s) is quite small, compared to the influence of heat flux (6.2 g/m^2-s), and does not affect the combustion mode like oxygen. Similarly, the model predicts a slight decrease in the burning rate with an increase in sample thickness (Fig. 11 c), meaning that all samples acted as thermally thick. Again, this variation (1 g/m^2-s) was small compared to the oxygen concentration and heat flux. The fitting correlations used in the simulations for experimental, ignition, and flaming time are summarized in Fig. 12. These findings imply that future experiments should continue to focus on heat flux and oxygen concentration.

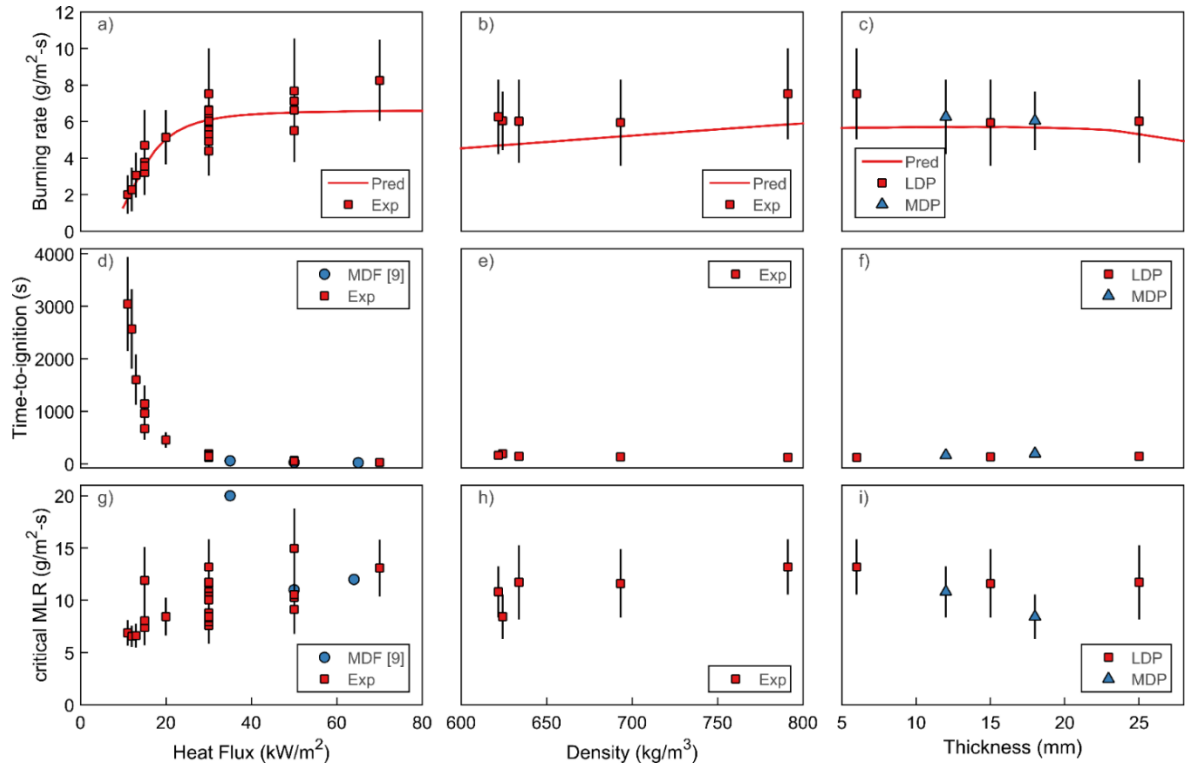

Fig. 11 Experimental and predicted data at different heat fluxes, density, and sample thickness. The average burning rate was determined from the full duration of experiments. The dependency of the experimental duration against each variable was found from the experiments through correlations.

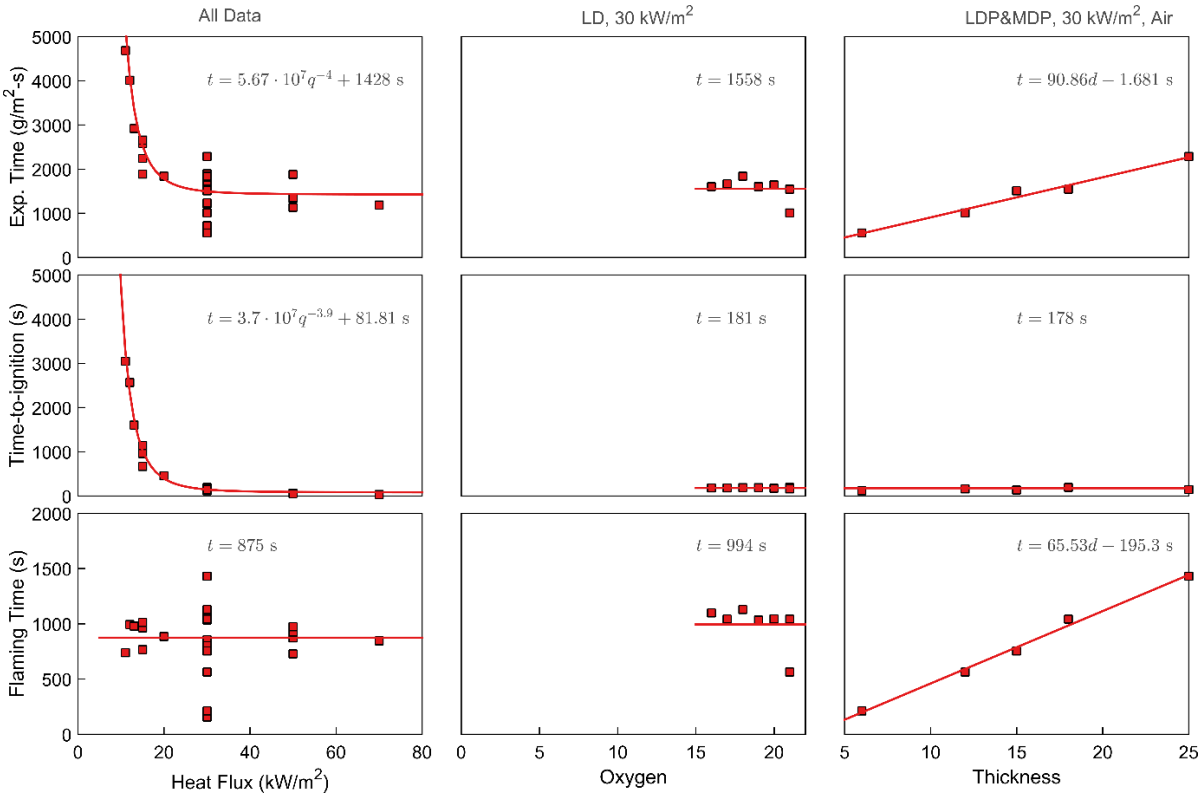

Fig. 12 The correlation between experimental time, time-to-ignition, and flaming time and heat flux, oxygen, and thickness used in the simulations are derived from the experimental measurement. The respective correlations are shown in each subplot.

This study has two potential limitations. The first limitation of our study is the extrapolation of our smouldering and flaming criticality. Hadden et al. [38] argued that the criticality of self-sustained smouldering is dependent on the fuel type, experimental set-up, and environmental variables. Subsequent studies, however, found different limiting oxygen concentrations (13.5 % in [44] and 10 % in [19]), meaning that the founded 4% limiting oxygen for smouldering wood depends on the heat flux, scale, and other parameters. Another limitation is that we restricted ourselves to one kind of engineered wood materials. However, all engineered woods are produced from natural wood and resin or glue. Their fundamental chemical composition and largely their microstructure should, therefore, be similar so that our results should hold, at least qualitatively, for most engineered woods.

4 Conclusions

In this paper, we characterised experimentally and computationally the influence of oxygen concentration and other variables on the burning of particleboard. Heat flux had a significant influence, while density and sample thickness had no effect on the burning rate and time-to-flaming ignition. Oxygen concentration controls the burning mode with pyrolysis dominating below 4 % $[O_2]_a$, smouldering between 4 and 15 % $[O_2]_a$, and flaming above 15 %. These thresholds agree with the literature. Comparing the mass loss rates at different oxygen concentrations revealed that flaming only enhanced the mass loss rates by 37 % compared to pure pyrolysis and smouldering. This finding leads us to the hypothesis that smouldering can lead to significant strength-loss in structural timber after flaming has ceased. Simultaneously studying the effect of heat flux and oxygen concentration on the ignition thresholds for smouldering and flaming ignition of wood demonstrated that the limited oxygen concentration (minimum oxygen concentration required for ignition) reduces with heat flux for both the smouldering and flaming. The analysis revealed, for the first time, a triple point for wood at which a small change in condition can lead to either smouldering, flaming, or pyrolysis. More importantly, smouldering causes the fire hazard of wood to be higher than anticipated near the triple point by providing a route for smouldering. Smouldering is currently not part of the fire safety design of timber buildings, and we, therefore, recommend revisiting this assumption. Smouldering combustion presents a danger and as a catalyst for flaming combustion. In summary, our paper provides the criticalities for each mode of combustion of wood, the first step towards studying the transition between them.

Acknowledgement

The authors thank EPSRC, Arup, and BRE Trust for financial support, and the University of Edinburgh for the experimental facilities used. Furthermore, we thank members of Imperial Hazelab for insightful discussions and helpful comments.

References

[1] S. Deeny, R.M. Hadden, A. Lawrence, B. Lane, Fire Safety Design in Modern Timber Buildings, Struct. Eng. 96 (2018) 48–53.

[2] W.C. Park, A. Atreya, H.R. Baum, Experimental and theoretical investigation of heat and mass transfer processes during wood pyrolysis, Combust. Flame. 157 (2010) 481–494.

[3] K. Li, X. Huang, C. Fleischmann, G. Rein, J. Ji, Pyrolysis of Medium Density Fibreboard: Optimized Search for Kinetic Scheme and Parameters via Genetic Algorithm Driven by Kissinger's Method, Energy & Fuels. (2014) 140822231738003.

[4] D. Zeinali, S. Verstockt, T. Beji, G. Maragkos, J. Degroote, B. Merci, Experimental study of corner fires—Part II: Flame spread over MDF panels, Combust. Flame. 189 (2018) 491–505.

[5] R.S. Miller, J. Bellan, A Generalized Biomass Pyrolysis Model Based on Superimposed Cellulose, Hemicellulos eand Liqnin Kinetics, Combust. Sci. Technol. 126 (1997) 97–137.

[6] G. Argawal, M. Chaos, Y. Wang, D. Zeinali, Pyrolysis model properties of Engineered Wood Products and validaton using Transient Heating scenarios, Interflam. (2016).

[7] K. Li, S. Hostikka, P. Dai, Y. Li, H. Zhang, J. Ji, Charring shrinkage and cracking of fir during pyrolysis in an inert atmosphere and at different ambient pressures, Proc. Combust. Inst. 000 (2016) 1–10.

[8] N. Boonmee, J.G. Quintiere, Glowing and flaming autoignition of wood, Proc. Combust. Inst. 29 (2002) 289–296.

[9] X. Huang, K. Li, H. Zhang, Modelling bench-scale fire on engineered wood: Effects of transient flame and physicochemical properties, Proc. Combust. Inst. 36 (2017) 3167–3175.

[10] J. Schmid, A. Santomaso, D. Brandon, U. Wickström, A. Frangi, Timber Under Real Fire Conditions – the Influence of Oxygen Content and Gas Velocity on the Charring Behavior, in: World Conf. Timber Eng., 2016.

[11] T.J. Ohlemiller, Forced smolder propagation and the transition to flaming in cellulosic insulation, Combust. Flame. 81 (1990) 354–365.

[12] G. Rein, Smoldering Combustion, in: SFPE Handb. Fire Prot. Eng., Springer New York, New York, NY, 2016: pp. 581–603.

[13] X. Huang, J. Gao, A Review of Near-Limit Opposed Fire Spread, Fire Saf. J. (2020).

[14] R. Crielaard, J.W. van de Kuilen, K. Terwel, G. Ravenshorst, P. Steenbakkers, Self-extinguishment of cross-laminated timber, Fire Saf. J. 105 (2019) 244–260.

[15] R. Emberley, T. Do, J. Yim, J.L. Torero, Critical heat flux and mass loss rate for extinction of flaming combustion of timber, Fire Saf. J. 1 (2017).

[16] D.J. Rasbash, B. Langford, Burning of wood in atmospheres of reduced oxygen concentration, Combust. Flame. 12 (1968) 33–40.

[17] C.M. Belcher, J.C. McElwain, Limits for Combustion in Low O2 Redefine Paleoatmospheric

Predictions for the Mesozoic, Science (80-.). 321 (2008) 1197–1200.

[18] J. Cuevas, J.L. Torero, C. Maluk, Flame extinction and burning behaviour of timber under varied oxygen concentrations, Fire Saf. J. (2020) 23.

[19] H. Wang, P.J. Van Eyk, P.R. Medwell, C.H. Birzer, Z.F. Tian, M. Possell, Effects of Oxygen Concentration on Radiation-Aided and Self-sustained Smoldering Combustion of Radiata Pine, Energy and Fuels. 31 (2017) 8619–8630.

[20] A.I. Bartlett, R.M. Hadden, L.A. Bisby, A Review of Factors Affecting the Burning Behaviour of Wood for Application to Tall Timber Construction, Fire Technol. 55 (2019) 1–49.

[21] F.X.J. Calle, Application of fire calorimetry to understand factors affecting flammability of cellulosic material: Pine needles, tree leaves and chipboard, 2012.

[22] C. Lautenberger, C. Fernandez-Pello, A model for the oxidative pyrolysis of wood, Combust. Flame. 156 (2009) 1503–1513.

[23] F. Richter, G. Rein, Heterogeneous kinetics of timber charring at the microscale, J. Anal. Appl. Pyrolysis. 138 (2019) 1–9.

[24] F. Richter, G. Rein, A multiscale model of wood pyrolysis in fire to study the roles of chemistry and heat transfer at the mesoscale, Combust. Flame. 216 (2020) 316–325.

[25] T. Kashiwagi, H. Nambu, Global kinetic constants for thermal oxidative degradation of a cellulosic paper, Combust. Flame. 88 (1992) 345–368.

[26] T.J. Ohlemiller, Smoldering combustion propagation through a permeable horizontal fuel layer, Combust. Flame. 81 (1990) 341–353.

[27] A. Anca-Couce, N. Zobel, A. Berger, F. Behrendt, Smouldering of pine wood: Kinetics and reaction heats, Combust. Flame. 159 (2012) 1708–1719.

[28] F. Richter, A. Atreya, P. Kotsovinos, G. Rein, The effect of chemical composition on the charring of wood across scales, Proc. Combust. Inst. 37 (2019) 4053–4061.

[29] X. Huang, G. Rein, Thermochemical conversion of biomass in smouldering combustion across scales: The roles of heterogeneous kinetics, oxygen and transport phenomena, Bioresour. Technol. 207 (2016) 409–421.

[30] T. Kashiwagi, T.J. Ohlemiller, K. Werner, Effects of external radiant flux and ambient oxygen concentration on nonflaming gasification rates and evolved products of white pine, Combust. Flame. 69 (1987) 331–345.

[31] G. Wu, D.U. Shah, E.R. Janeček, H.C. Burridge, T.P.S. Reynolds, P.H. Fleming, P.F. Linden, M.H. Ramage, O.A. Scherman, Predicting the pore-filling ratio in lumen-impregnated wood, Wood Sci. Technol. 51 (2017) 1277–1290.

[32] X. Huang, G. Rein, H. Chen, Computational smoldering combustion: Predicting the roles of moisture and inert contents in peat wildfires, Proc. Combust. Inst. 35 (2015) 2673–2681.

[33] M. Zarzecki, J.G. Quintiere, R.E. Lyon, T. Rossmann, F.J. Diez, The effect of pressure and oxygen concentration on the combustion of PMMA, Combust. Flame. 160 (2013) 1519–1530.

[34] D.E. Ward, C.C. Hardy, Smoke emissions from wildland fires, Environ. Int. 17 (1991) 117–134.

[35] W.C. Park, A. Atreya, H.R. Baum, Determination of pyrolysis temperature for charring materials, Proc. Combust. Inst. 32 (2009) 2471–2479.

[36] T.J. Ohlemiller, Modeling of smoldering combustion propagation, Prog. Energy Combust. Sci. 11 (1985) 277–310.

[37] M.G. Ortiz-Molina, T.Y. Toong, N.A. Moussa, G.C. Tesoro, Smoldering combustion of flexible polyurethane foams and its transition to flaming or extinguishment, Symp. Combust. 17 (1979) 1191–1200.

[38] R.M. Hadden, G. Rein, C.M. Belcher, Study of the competing chemical reactions in the initiation and spread of smouldering combustion in peat, Proc. Combust. Inst. 34 (2013) 2547–2553.

[39] F. Wiesner, L.A. Bisby, A.I. Bartlett, J.P. Hidalgo, S. Santamaria, S. Deeny, R.M. Hadden, Structural capacity in fire of laminated timber elements in compartments with exposed timber surfaces, Eng. Struct. 179 (2019) 284–295.

[40] H. Kinjo, Y. Katakura, T. Hirashima, S. Yusa, K. Saito, Deflection behavior and load-bearing period of structural glued laminated timber beams in fire including cooling phase, J. Struct. Fire Eng. 9 (2018) 287–299.

[41] A. Bartlett, F. Wiesner, R. Hadden, L. Bisby, B. Lane, A. Lawrence, P. Palma, A. Frangi, Needs for total fire engineering of mass timber buildings, WCTE 2016 - World Conf. Timber Eng. (2016).

[42] K. Miyamoto, X. Huang, N. Hashimoto, O. Fujita, C. Fernandez-Pello, Limiting oxygen concentration (LOC) of burning polyethylene insulated wires under external radiation, Fire Saf. J. 86 (2016) 32–40.

[43] N. Bal, Forty years of material flammability: An appraisal of its role, its experimental determination and its modelling, Fire Saf. J. 96 (2018) 46–58.

[44] J. Yang, N. Liu, H. Chen, W. Gao, R. Tu, Effects of atmospheric oxygen on horizontal peat smoldering fires: Experimental and numerical study, Proc. Combust. Inst. 37 (2019) 4063–4071.